13 Estimating Actual Evapotranspiration from Irrigated Fields Using a Simplified Surface Energy Balance Approach

Gabriel B. Senay, Michael E. Budde, James P. Verdin, and James Rowland
U.S. Geological Survey Earth Resources Observation and Science Centre

CONTENTS

13.1 INTRODUCTION

Food security assessment in many developing countries, such as Afghanistan, is vital because the early identification of populations at risk can enable the timely and appropriate actions needed to avert widespread hunger, destitution, or even famine. The assessment is complex, requiring the simultaneous consideration of multiple socioeconomic and environmental variables. Since large and widely dispersed

populations depend on rain-fed and irrigated agriculture and pastoralism, large-area weather monitoring and forecasting are important inputs to food security assessments. The Famine Early Warning Systems Network (FEWS NET), an activity funded by the United States Agency for International Development (USAID), employs a crop water balance model (based on the water demand and supply at a given location) to monitor the performance of rain-fed agriculture and forecast relative production before the end of the crop-growing season. While a crop water balance approach appears to be effective in rain-fed agriculture [1,2], irrigated agriculture is best monitored by other methods, since the supply (water used for irrigation) is usually generated from upstream areas, farther away from the demand location.

13.2 BACKGROUND

Several researchers [3–7] have successfully applied the surface energy balance method to estimate crop water use in irrigated areas. Their approach requires solving the energy balance equation at the surface (Equation 13.1) where the actual evapotranspiration (ETa) is calculated as the residual of the difference between the net radiation to the surface and losses due to the sensible heat flux (energy used to heat the air) and ground heat flux (energy stored in the soil and vegetation).

$$LE = Rn - G - H, \tag{13.1}$$

where:

LE = latent heat flux (energy consumed by ETa) (W/m^2),
Rn = net radiation at the surface (W/m^2),
G = ground heat flux (W/m^2),
H = sensible heat flux (W/m^2).

The estimation of each of these terms from remotely sensed imagery requires quality data sets. Allen et al. [6] described well the various steps required to estimate ETa using the surface energy balance method, which employs the *hot* and *cold* pixel approach by Bastiaanssen et al. [3]. In summary, for the net radiation, data on incoming and outgoing radiation and the associated surface albedo and emissivity fractions for shortwave and longwave bands are required. The ground heat flux is estimated using surface temperature, albedo, and Normalized Difference Vegetation Index (NDVI). The sensible heat flux is estimated as a function of the temperature gradient above the surface, surface roughness, and wind speed.

13.3 RATIONALE

While solving the full energy-balance equation has been shown to give good results in many parts of the world, the data and skill requirements to solve the various

terms in the equation are prohibitive for operational applications in large regions where anomalies are more useful than absolute values. In this study, we implemented a Simplified surface energy balance (SSEB) approach [8] to estimate ETa, which maintains and extends the major assumptions in the Surface Energy Balance Algorithm for Land (SEBAL [3]) and the Mapping ETa at High Resolution using Internalized Calibration (METRIC [6]). Both SEBAL and METRIC assume that the temperature difference between the land surface and the air (near-surface temperature difference) varies linearly with land surface temperature (LST). They derive this relationship based on two anchor pixels, known as the hot and cold pixels, representing dry and bare agricultural fields and wet and well-vegetated fields, respectively. SEBAL and METRIC methods use the linear relationship between the near-surface temperature difference and the LST to estimate the sensible heat flux, which varies as a function of the near-surface temperature difference, by assuming that the hot pixel experiences no latent heat, i.e., ET = 0.0, whereas the cold pixel achieves maximum ET.

The SSEB modeling approach extends this assumption with a further simplification by stating that the latent heat flux (ETa) also varies linearly between the hot and cold pixels. This assumption is based on the logic that temperature difference between soil surface and air is linearly related to soil moisture [9]. On the other hand, crop soil water balance methods estimate ETa using a linear reduction from the potential ET, depending on soil moisture [2,10]. Therefore, we argue that ETa can be estimated by the near-surface temperature difference, which in turn is estimated from the land surface temperatures (LSTs) of the hot and cold pixels in the study area. In other words, while the hot pixel of a bare agricultural area experiences little ET and the cold pixel of a well-watered irrigated field experiences maximum ET, the remaining pixels in the study area will experience ET in proportion to their LST in relation to the hot and cold pixels. This approach can be compared to the Crop Water Stress Index (CWSI) first developed by Jackson [11]. The CWSI is derived from the temperature difference between the crop canopy and the air. Dividing the current temperature difference with known upper and lower canopy air temperature values creates a ratio index varying between 0 and 1. The lower-limiting canopy temperature is reached when the crop transpires without water shortage, while the upper-limiting canopy temperature is reached when the plant transpiration is zero due to water shortage [12]. In this study, the *cold* and *hot* anchor LST pixel values can be compared to the equivalent of the lower- and upper-limiting canopy temperatures, respectively, of the CWSI method.

13.4 GOALS

The main objective of this study was to produce ETa estimates using a combination of ET fractions (ETfs) generated from (Moderate Resolution Imaging Spectroradiometer) MODIS thermal imagery and global reference ET data over known irrigated fields in Afghanistan.

13.5 METHODS

13.5.1 Study Area

The study site is located in the Baghlan province of North-central Afghanistan, as shown in Figure 13.1. A polygon was defined around an irrigated area (Figure 13.1) using a combination of Landsat and MODIS data sets. The total area of the polygon is approximately 62,400 hectares and consists of both well-vegetated and sparsely vegetated areas, with some arid/semiarid areas at the periphery of the polygon.

13.5.2 Data

The primary data sets for this study were derived from the MODIS sensor flown onboard the Terra satellite. MODIS LST data were used to calculate the crucial ETfs explained in Section 13.5.3. Additionally, MODIS NDVI data were used for irrigated area delineation and identifying highly vegetated vs. sparsely vegetated areas within the agricultural zone. The global reference ET data were obtained from the archives of United States Geological Survey (USGS)/FEWS NET operational model outputs. Each data set is further described below.

13.5.2.1 MODIS Land Surface Temperature

Thermal surface measurements were collected from the MODIS eight-day LST/Emissivity (LST/E) product (MOD11A2). The MODIS instrument provides 36 spectral bands, including 16 in the thermal portion of the spectrum. The LST/E

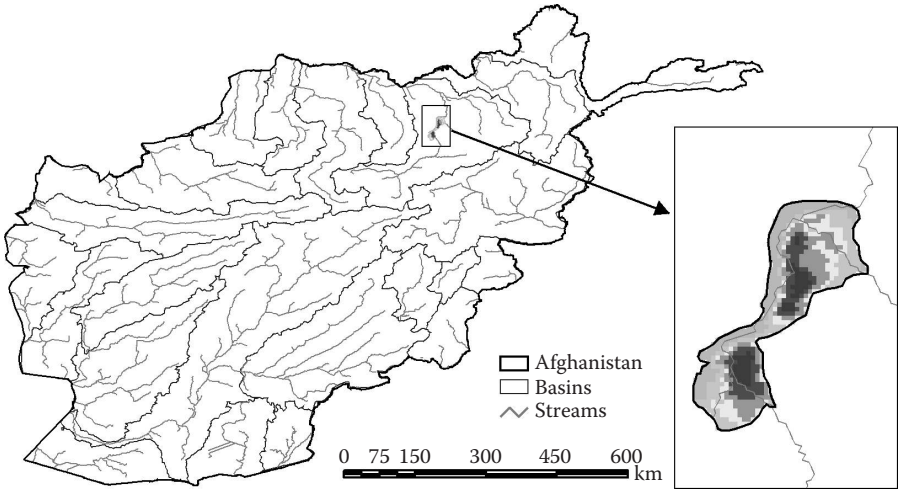

FIGURE 13.1 Study site showing the irrigated fields in the Baghlan province with a network of streams and drainage basins. The streamflow within the basin that includes our study area is northward, originating from the central highlands.

products provide per-pixel temperature and emissivity values at 1-km spatial resolution for eight-day composite products and 5-km resolution for daily products. Temperatures are extracted in degrees Kelvin with a view-angle dependent algorithm applied to direct observations. This study utilized eight-day average daytime LST measurements for eight-day composite periods throughout the growing season. Table 13.1 shows the MODIS composite day representing the first day of the eight-day MODIS LST composite period and corresponding calendar dates. Although MODIS thermal data are available on a daily time step, we used the average daytime LST measurements for eight-day composite periods in order to minimize the effects of cloud contamination on daily observations. We believe that the eight-day composites do not compromise our ability to accurately represent surface temperature conditions that occur before and after irrigation applications during the composite period.

13.5.2.2 MODIS Vegetation Index (VI)

MODIS Vegetation Index (VI) products use reflectance measures in the red (620–670 nm), near infrared (841–876 nm), and blue (459–479 nm) bands to provide spectral measures of vegetation greenness. The MODIS VI products include the standard NDVI and the Enhanced Vegetation Index (EVI). Both indices are available at 250-m, 500-m, and 1-km spatial resolution. The primary difference between the two indices is that EVI uses blue reflectance to provide better sensitivity in high biomass regions. Since this study concentrated on irrigated agriculture in an otherwise dryland environment, we used the NDVI product at 250-m resolution for this analysis.

These data are distributed by the Land Processes Distributed Active Archive Center, located at the U.S. Geological Survey's EROS http://LPDAAC.usgs.gov.

13.5.2.3 Reference ET

The global one-degree reference ET (ETo), based on the six-hourly Global data assimilation systems (GDAS) model output, is calculated daily at the Earth Resources Observation and Science (EROS) Center on an operational basis [13]. The

TABLE 13.1
MODIS Composite Day and Corresponding Calendar Dates for each Growing Season

MODIS Composite Day	161	177	193	209	225	241
2000, 2004	9–16 June	25 June to 2 July	11–18 July	27 July to 3 August	12–19 August	28 August to 4 September
2001, 2002, 2003	10–17 June	26 June to 3 July	12–19 July	28 July to 4 August	13–20 August	29 August to 5 September

GDAS ETo uses the standard Penman–Monteith equation, as outlined in the FAO publication for short-grass reference ETo by Allen et al. [10]. The feasibility of using the GDAS ETo for such applications was recommended by Senay et al. [13] after a comparison with station-based daily ETo showed encouraging results with r^2 values exceeding 0.9. Daily global reference ET values were available for all days between 2001 and 2004. For 2000, the daily reference ET values were not complete. This study used six thermal image dates during the main growing season. Three of the six image dates in 2000 did not have a corresponding reference ET. For the missing time periods, the average reference ET from 2001 to 2004 was used.

13.5.3 Descriptions of Methods

A set of three hot and three cold pixels were selected for each eight-day composite period for each year of the growing season data. An average of the three pixels was used to represent the *hot* and *cold* values throughout the study area. The pixels were selected using a combination of MODIS 250-m NDVI, MODIS LST, and Landsat ETM + imagery when available. For a given time period, cold pixels, representing well-vegetated and well-watered crops, were selected based on either visual interpretation of the Landsat imagery or high values in the MODIS NDVI. Similarly, hot pixels representing low-density vegetation and relatively dryland were identified either visually or by selecting pixels with very low NDVI values. LST data were used to verify that the selected pixels adequately represented the temperature contrast within the study area for each eight-day composite period.

LST values for each of the six pixels (three hot, three cold) were extracted using ArcGIS software [14]. The resulting database files were imported into an Excel spreadsheet, where average hot and cold pixel values were calculated.

Since we know that hot pixels experience very little ET and cold pixels represent maximum ET throughout the study area, the average temperature of hot and cold pixels could be used to calculate proportional fractions of ET on a per-pixel basis. The ET fraction (ETf) was calculated for each pixel by applying Equation 13.2 to each of the eight-day MODIS LST scenes.

$$\mathrm{ETf} = \frac{\mathrm{TH} - \mathrm{Tx}}{\mathrm{TH} - \mathrm{TC}}, \tag{13.2}$$

where TH is the average of the three hot pixels selected for a given scene, TC is the average of the three cold pixels selected for that scene, and Tx is the LST value for any given pixel in the composite scene.

The ETf formula was applied to the six eight-day growing season composites for each year, resulting in a series of six images per season. The images contained ETfs for each pixel that were used to estimate ETa throughout the growing season.

The ETf is used in conjunction with a reference ET (ETo) to calculate the per-pixel ETa values in a given scene. The reference ETo is calculated on both daily and dekadal (ten-day) time steps for the globe at one-degree spatial resolution. The

dekadal period that corresponded closest to the eight-day MODIS composite period was used to extract average daily ETo values by dividing the dekadal sum into ten daily values. Since our analysis uses every other eight-day period between June and September, each composite period essentially represents the 16 days between observations. Thus, the average daily reference ETo values were multiplied by 16 to provide a summation of ETo for each 16-day period. The calculation of ETa was achieved using the following formula:

$$\mathrm{ETa} = \mathrm{ETf} * \mathrm{ETo}. \tag{13.3}$$

This simplified energy balance approach allowed us to use known reference ET at a coarse spatial resolution of one-degree to derive spatially distributed ET measurements based on LST variability at 1-km resolution. Improvements in the spatial representation of ET distribution during the growing season can provide important insights into the extent of irrigated crop areas and the quality of the growing season.

Actual crop ET for the five-year period, 2000–2004, was used to assess the quality of each growing season in the North-central Afghanistan study area. Using a mask of the irrigated crop area, described in Figure 13.1, we used the actual 1-km gridded ET values to calculate spatially averaged ET for each season. Furthermore, the results from the SSEB model were compared to a watershed-based analysis of an operational FEWS NET irrigation supply and demand model. The irrigation supply and demand model has been using satellite-derived rainfall and GDAS ETo for modeling growing seasons since 1996, and average supply and demand is determined using monthly climatological data defined using a 30-year monthly rainfall and potential ET from 1961 to 1990 (www.cgiar.org/iwmi/WAtlas/atlas.htm). The results and implications of these comparisons are outlined in detail in the following sections.

13.6 RESULTS AND DISCUSSIONS

The results of the analysis are presented in Figures 13.2 through 13.7. Figure 13.2 shows the hot and cold pixel values for the six time-periods used for 2003. Similar temporal patterns were also observed in the other years. For 2003, the hot and cold pixels were separated by an average of approximately 15°C throughout the season between June and August. Furthermore, they appeared to increase or decrease in the same direction by about the same magnitude during the peak portion of the crop-growing season. However, this separation approaches close to 0.0 (data not shown) during the off-seasons, particularly close to the start of the season. The existence of such temporal patterns between the hot and cold pixels is believed to be potentially useful in detecting time of start of season for crop-monitoring activities. Figure 13.2 shows the boundary (extreme) conditions for surface temperature distribution in the study site for each of the growing seasons. By properly selecting the extreme temperature areas representing the hot (dry/bare) and the cold (wet/vegetated) land areas, the remaining pixels in the study area will fall in between these temperature values. The two extreme temperatures also represent extremes in ET values. The range of these values varies from zero ET for the *hot* and dry areas to a high ET, comparable

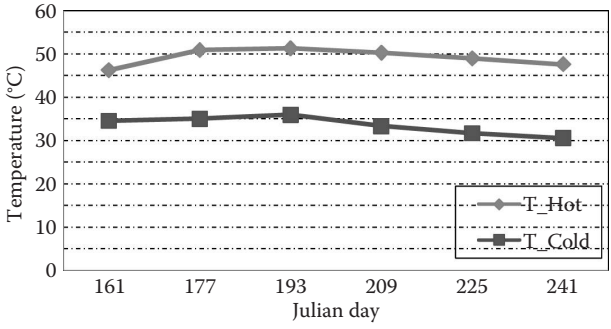

FIGURE 13.2 Temporal variation of the average *hot* and *cold* pixel land surface temperature values during the 2003 crop growing season in °C.

to a reference ET, for the *cold* and wet areas [6]. In this study, we extended this assumption to include the remaining pixels by suggesting that pixels having LST values in between these extremes will experience an ET value in direct proportion to the ETf, as shown in Equation 13.2. One of the challenges of this method is the subjectivity of selecting the hot and cold pixels that truly represent the effect of soil moisture and prevailing climatic conditions of the study area. Although it is harder to find hot pixels with zero evaporation, this problem is less pronounced in irrigated areas than in rain-fed areas where soil moisture can be replenished by rainfall during the eight-day period. We recommend the approach of Allen et al. [6] to determine ETa of the hot pixel using a water balance model for bare soil if rainfall has occurred during the eight-day period.

Figure 13.3 shows the temporal trend of spatially averaged ETfs during the peak-growing season for each of the 5 years used in this study. The ETfs showed both intraseasonal and interseasonal variability of up to 20% from their respective mean values. The major separation between the different years was shown in the middle of the peak season for composite periods beginning on days 193 and 209 (Figure 13.3) when the spatially averaged ETf appears to be lowest. The relatively high ETf in the beginning of the season may be explained by the fact that there is more higher ground cover condition across the study site with the presence of other vegetation that takes advantage of the spring rainfall in addition to crops planted for irrigation. As shown in Figure 13.2, the separation between the *hot* and *cold* pixels on day 161 is the smallest. This suggests that early in the season there are more pixels closer to the *cold* pixel than the *hot* pixel when compared to the remainder of the season. This may be due to the accumulated moisture from the preceding spring, even in nonirrigated areas that would run out of moisture during the remainder of the summer unlike the irrigated areas.

Figure 13.4 shows daily reference ET values that correspond to ETfs from Figure 13.3. For the majority of the points, the daily reference ET varied between 6 and 8 mm per day. Unlike the ETf in Figure 13.3, the reference ET values did not show a marked difference from year to year in any particular time period, with the exception of the 2003 reference ET, which showed distinctly higher ETo values for days 193 and 209. The 2003 data suggest that the region benefited from two important

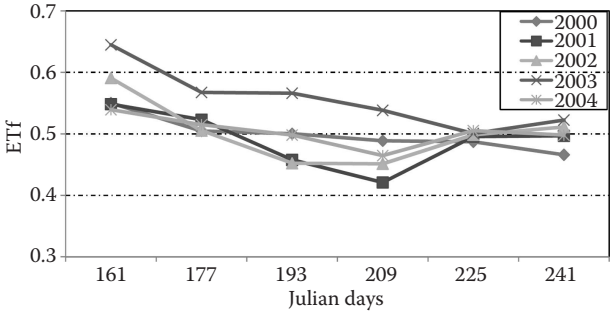

FIGURE 13.3 Temporal patterns of spatially averaged ET fractions for peak-season (June 10 to August 29) 2000–04.

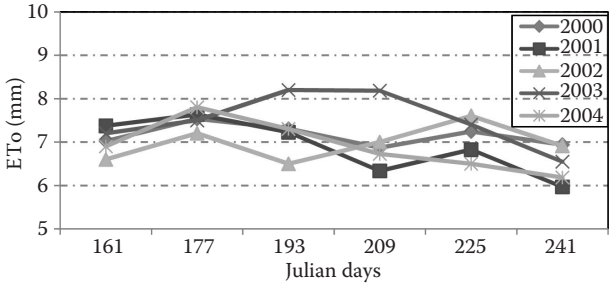

FIGURE 13.4 Temporal patterns of spatially averaged daily reference ET for peak-season (June 10 to August 29) 2000–04.

factors during the 2003 crop-growing season: (1) good water supply as evidenced by the high ETfs; and (2) good energy supply and vapor transport mechanism (clear sky, favorable wind) as evidenced by the high reference ET, which is mainly a measure of the available energy and vapor transport mechanism under optimum water supply conditions.

The actual crop ET is estimated from the product of ETf and the reference ET, as shown by Equation 13.3. Figure 13.5 shows the temporal patterns of the actual crop ET for the five periods. Each data point represents a 16-day ETa estimate that is spatially averaged over the study area. Due to the small size of the study area compared to the spatial resolution of the reference ET, all pixels in the study area have an identical reference ET value for each of the six image dates. Thus, the spatial variation in the ETa is a result of the spatial variation of the ETfs. The spatially averaged seasonal ETa magnitudes are presented in Figure 13.6 to illustrate the year-to-year variability in ETa. Figure 13.6 highlights the fact that 2003 was the best agricultural season during the five-year period, which is corroborated by various field reports that the cycle of three consecutive drought periods, between 2000 and 2002, was alleviated by good precipitation in the 2003 season. These results are comparable to a watershed-based analysis of an operational FEWS NET irrigation supply and demand model output, showing that 2002 and 2004 had below-average supply while the 2003 irrigation water supply met the average demand.

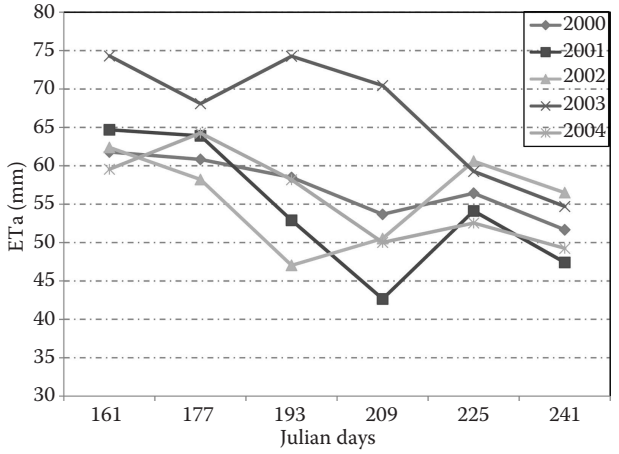

FIGURE 13.5 Temporal patterns of spatially averaged 16-day actual ET for peak-season (June 10 to August 29) 2000–04.

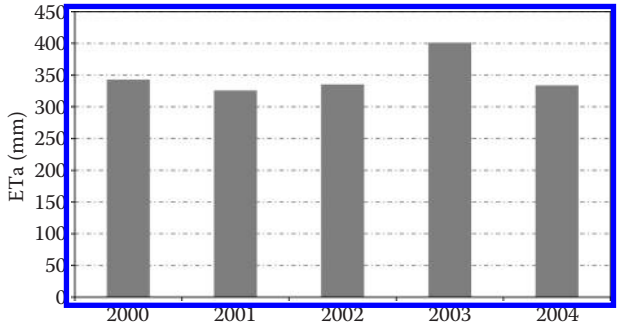

FIGURE 13.6 Spatially averaged peak season (96 days: June 2 to September 6) actual crop ET (mm) from 2000 to 04.

While Figures 13.3 through 13.6 show spatially averaged temporal variation of the ETfs, reference ET, and ETa, Figure 13.7a and b present the spatial variation of the seasonal ETa for 2002 and 2003, respectively. As shown in Figure 13.6, the higher values of the 2003 seasonal ET are illustrated by the expanded extent of higher ETa classes (dark green colors) compared to the 2002 ETa map. A similar pattern of expansion/reduction in greenness for the corresponding years was observed from MODIS seasonal maximum NDVI data. The reduction in ETa values in 2002 has mainly occurred in the downstream irrigated fields (northern fields) where a short tributary joins the main river. The geographic area where lower ETa values were observed seems to suggest downstream irrigators/fields would have access to water only if there was a surplus over the demands of the upstream users. This is more in line with a common practice in regions where water rights are not well established or regulated. Furthermore, Figure 13.7a and b suggest the possibility of using this method of analysis to estimate harvested irrigated areas for a given year based on a threshold of ETa required for successful crop growth. For example,

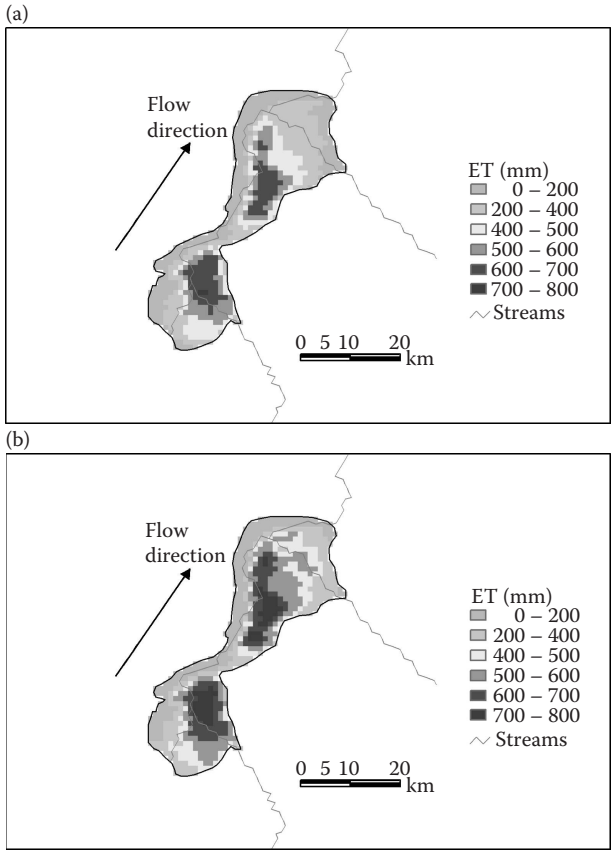

FIGURE 13.7 **(See color insert following page 256.)** (a) Seasonal (June 2 to September 6) actual ET distribution in irrigated fields of the study area in 2002. Arrow indicates the general south-north flow direction of the streams. (b) Seasonal (June 2 to September 6) actual ET distribution in irrigated fields of the study area in 2003. Arrow indicates the general south-north flow direction of the streams.

in the study area where certain fields consumed up to 700 mm in about 3 months, areas that only used half (350 mm) of the water demand by a well-watered crop could be considered as unsuccessful and removed from harvested irrigated areas [1,2,15]. Although the accuracy of the magnitudes of the estimated ETa values requires field validation using other methods or field studies, the methodís relative performance in terms of capturing the year-to-year variability suggests that the method has a potential to characterize irrigated field crop performance in relative terms on reasonably homogeneous flat irrigated fields. Although seasonal ETa values can be a surrogate for crop production, historical crop yield and production data are required to develop a statistical relationship between the two. Without field data, we can only present relative changes in water use that would also indicate directional changes in production. In order to improve the accuracy of ETa magnitude estimates, a method is being developed to downscale the coarser reference ETo to 10 km.

13.7 CONCLUSIONS

The main objective of this study was achieved with the demonstration of the successful application of the SSEB approach using MODIS thermal data sets in producing ETa estimates in an irrigated agricultural area of Afghanistan. The ETa values of the irrigated fields in the study area showed year-to-year variability that was consistent with field reports and other independent data sets, such as the seasonal maximum NDVI and output from an irrigation supply/demand water balance model. Particularly, the 2003 seasonal ETa of the study area was much higher than the rest of the studied years, and about 15% more than the average of the five years. This was in agreement with published reports [16] and news sources that stated 2003 precipitation appeared to have broken the spell of the preceding consecutive dry years in Afghanistan.

A close examination of the spatial distribution of the ETa estimates during 2003 and 2002 revealed that the reduction in area of high ETa values during 2002 was in the downstream part of the basin. Since this corresponds to a common practice where water is generally used first by those upstream, the result reinforces the reliability of this approach and points to the potential application of this method for spatially estimating cropped area in irrigated fields. The existence of a variable temporal pattern between the *hot* and *cold* pixels during the crop season is also believed to be potentially useful in detecting the time of start of season for crop-monitoring activities.

A more recent and ongoing evaluation of the SSEB approach in the United States has shown that SSEB ETa estimates compared well with Lysimeter data and ETa output from the METRIC model. Thus, the results of this study demonstrate the potential of applying the SSEB approach in different parts of the world, especially in remote locations where field-based information is not readily available.

REFERENCES

1. Verdin, J. and Klaver, R., Grid cell based crop water accounting for the famine early warning system, *Hydrological Processes*, 16, 1617–30, 2002.
2. Senay, G.B. and Verdin, J., Characterization of yield reduction in Ethiopia using a GIS-based crop water balance model, *Canadian Journal of Remote Sensing*, 29, 6, 687–92, 2003.
3. Bastiaanssen, W.G.M. et al., A remote sensing surface energy balance algorithm for land (SEBAL): 1) Formulation, *Journal of Hydrology*, 212, 213, 213–29, 1998.
4. Bastiaanssen, W.G.M. et al., SEBAL model with remotely sensed data to improve water resources management under actual field conditions, *Journal of Irrigation and Drainage Engineering*, 131, 1, 85–93, 2005.
5. Bastiaanssen, W.G.M., SEBAL-based sensible and latent heat fluxes in the irrigated Gediz Basin, Turkey, *Journal of Hydrology*, 229, 87–100, 2000.
6. Allen, R.G. et al., A Landsat-based energy balance and evapotranspiration model in Western US Water Rights Regulation and Planning, *Journal of Irrigation and Drainage Systems*, 19, 3–4, 251–268, 2005.
7. Su, H. et al., Modeling evapotranspiration during SMACEX, comparing two approaches for local and regional scale prediction, *Journal of Hydrometeorology*, 6, 6, 910–22, 2005.

8. Senay, G.B. et al., A coupled remote sensing and simplified surface energy balance approach to estimate actual evapotranspiration from irrigated fields, *Sensors*, 7, 979–1000, 2007.
9. Sadler, E.J. et al., Site-specific analysis of a droughted corn crop, water use and stress, *Agronomy Journal*, 92, 403–10, 2000.
10. Allen, R.G. et al., *Crop Evapotranspiration*, Food and Agriculture Organization of the United Nations, Rome, Italy, 1998.
11. Jackson, R.D., Canopy temperature and crop water stress, in *Advances in Irrigation*, D. Hillel (Ed.), Vol. 1., Academic Press, New York, 1982, 43–85.
12. Qiu, G.Y. et al., *Detection of Crop Transpiration and Water Stress by Temperature Related Approach under Field and Greenhouse Conditions*, Department of Land Improvement, National Research Institute of Agricultural Engineering, Tsukuba, Ibraki, Japan, 1999.
13. Senay, G.B. et al., Global reference evapotranspiration modeling and evaluation, *Journal of American Water Resources Association*, 44, 3, 1–11, 2008.
14. ESRI (Environmental Systems Research Institute), *ArcGIS 9.0.*, Environmental Systems Research Institute, Redlands, CA, 2004.
15. Doorenbos, J. and Pruitt, W.O., *Crop Water Requirements*, FAO Irrigation and Drainage Paper No. 24, Food and Agriculture Organization of the United Nations, Rome, Italy, 1977.
16. FEWS NET (Famine Early Warning System Network), *Afghanistan Monthly Food Security Bulletin*, September, 2003 (www.fews.net).